An L-band Brightness Temperature Disaggregation Method using S-band Radiometer Data for the Water Cycle Observation Mission (WCOM)

Panpan Yao[1,4,5], Jiancheng Shi[2,4], Tianjie Zhao[2,4], Michael H.Cosh[5] , Rajat Bindlish[6] and Hui Lu[1,4]

[1] *Ministry of Education Key Laboratory for Earth System Modeling, and Department of Earth System Science, Tsinghua University, Beijing 100084, China; yaopp@radi.ac.cn*

[2] *State Key Laboratory of Remote Sensing Science, Institute of Remote Sensing and Digital Earth, Chinese Academy of Sciences, Beijing 100101, China; shijc@radi.ac.cn, zhaotj@radi.ac.cn.;*

[3] *Graduate School of University of Chinese Academy of Sciences, Beijing 100049; China*

[4] *The Joint Center for Global Change Studies, Beijing 100875, China;*

[5] *USDA ARS Hydrology and Remote Sensing Laboratory, Beltsville, MD 20705, USA; Michael.Cosh@ars.usda.gov*

[6] *NASA/GSFC, Greenbelt, MD 20771, USA; rajat.bindlish@nasa.gov*

Abstract—The Water Cycle Observation Mission (WCOM) will build upon previous L and C band passive microwave soil moisture satellite missions. WCOM will consist of a passive microwave synthetic aperture radiometer operating at L, S, and C bands. The WCOM requirements for passive soil moisture are to estimate soil moisture in the top 5 cm of soil layer with an error less than 0.04 m^3/m^3, at 15 km resolution and with a 3-day revisit. A new set of algorithms for these multi-frequency platforms will need to be developed for estimating the data products at the desired resolution. To accomplish this, a brightness temperature (TB) downscaling methodology is developed that uses passive S-band TB (30 km) to downscale L-band TB (50 km) and to estimate soil moisture at a 30 km resolution, based on the linear relationships between the passive signals of L-band and S-band. To test this downscaling method, analysis was performed using PALS data from the Soil Moisture Experiments in 2002 (SMEX02). For this study, 4 km L-band observations were downscaled to 800 m. The root mean square errors (RMSE) between the downscaled TBL at 800m with the observed TBL at 800m are 2.63 K and 1.60 K for H and V polarizations respectively. The results also showed that it was possible to use these disaggregated TB to estimate soil moisture to meet the mission requirement of 0.04 m^3/m^3. These results showed that we can obtain higher resolution soil moisture from L band passive TB with a high accuracy (<0.04 m^3/m^3) by using S-band information.

Index Terms—Brightness Temperature, Disaggregation, Passive microwave, Soil moisture.

I. INTRODUCTION

Soil moisture is of great importance to enhance understanding the land-atmosphere fluxes in energy, water, and carbon cycle. Soil moisture has various applications that can have major influence on human society and environment, such as drought and flood prediction, water resources management, agricultural production, weather forecasting and climate change[1][2][3]. Thus, accurate and high resolution global mapping of soil moisture is vital to satisfy the need of these applications.

For remote sensing measurements of soil moisture, there has been a great interest in L-band radiometers in recent years[4] with the launch of several new satellites platform including L band sensors, due to the deeper observation depth and decreased ancillary effects of atmosphere and vegetation. The Soil Moisture and Ocean Salinity (SMOS) mission was launched by European Space Agency on November 2, 2009[5][6]. It is the first mission to provide global microwave brightness temperature observations at L-band, dedicated to soil moisture and ocean salinity with dual polarizations and a wide range of incidence angles (5°~60° approximately). Aquarius/SAC-D (a NASA joint project with Argentina) combines passive/active L-band microwave instruments[7] to provide accurate measurements of ocean salinity (the primary objective of the mission) and land surface soil moisture[8]. The Soil Moisture Active Passive (SMAP) mission was launched by National Aeronautics and Space Administration (NASA)on January 31, 2015 [9]. It provides higher resolution of global soil moisture by combining measurements of L-band brightness temperature and backscatter at a single incidence angle of 40°. All these L-band satellites can provide soil moisture products with 40 km resolution. However, higher resolution products are required to meet the need of hydrometeorology, ecology, water resources management, and agricultural applications [10]. China is proposing a Water Cycle Observation Mission (WCOM) to combine active and passive microwave simultaneous measurements on the key elements of land, sea, and atmosphere, which will include a passive radiometer operating at L, S, and C bands[11][12]. The WCOM passive sensor requirements for soil moisture are to estimate soil moisture in the top 5 cm of soil layer with an error less than 0.04 m^3/m^3, at 15 km resolution and with 3-day revisit. The microwave radiometer signals provided by L-band are sensitive to soil moisture in regions with medium vegetation water contents (VWC) at coarse resolution (50 km). The S-band and C-band provide TB measurements at higher resolution (30 km/15 km) with limited soil moisture retrieval accuracy.

This study presents a passive-only TB downscaling method

according to the unique configuration of WCOM multichannel passive observations. It will be evaluated against a field experiment data set which was collected in 2002 with both sets of L-band and S-band data. This paper is organized as follows: Section 2 introduces the WCOM mission and its passive payload, as well as the advantages to downscaling. Section 3 is an experimental study using field data. Section 4 describes the theoretical basis of the downscaling methods. Section 5 is the passive-only TBs downscaling results and discussion. Finally, Section 6 summarizes the conclusions.

II. WCOM OVERVIEW

WCOM is the first planned earth science satellite mission of China, with the most synergistic capabilities for global water cycle observations. It will provide accurate measurements of key elements of the global water cycle, including the soil moisture, freeze/thaw state, ocean salinity, snow water equivalent, atmospheric water vapor, precipitation and other associated parameters. Water cycle study is a global issue of great science importance, which describes the movement, phase and storage of water and plays a major role in the earth system. Satellite remote sensing observations are the only reliable techniques for obtaining global estimates of soil moisture. The overall scientific objectives of the WCOM mission are: (1) To significantly improve the accuracy and synchronization of measurements for spatial and temporal distribution of global water cycle key elements and system, (2) To refine the long-term satellite observations over past decades, and to provide a new opportunity to improve water cycle related model.

To understand the needs of the downscaling algorithm, it is first necessary to review the principles of future remote sensing datasets which will need this algorithm. The WCOM satellite will be flown with a 6:00 am/pm sun synchronous polar orbit at 600 km height, to make the surface resolution and satellite power feasible.

Table 1. Payloads of WCOM

Payloads	IMI	PMI	DFPSCAT
Frequency(GHz)	L/S/C (1.4/2.4/7.2)	C~W(6.8,10.65,18.7, 23.8,37,89)	X, Ku (9.6,14/17)
Spatial Resolution(km)	50/30/15	4~50(frequencies)	2~5(processed)
Swath Width(km)	>1000	>1000	>1000
Polarization	Full-Pol	Full-Pol	Full-Pol
Sensitivity	0.1~0.2K	0.3~0.5K	0.5dB
Temporal Resolution(Day)	2~3	2~3	2~3

There will be three microwave payloads on the WCOM (Table 1). The first sensor is a full polarized interferometric imager (IMI) operating at L-, S-, and C-band frequencies with spatial resolution of 50 km/30 km/15 km respectively. This sensor is mainly designed for observing soil moisture and sea salinity. It consists of a 9 m by 6 m mesh reflector and one-dimensional thinned array as the feed. The second sensor is a polarized microwave radiometric imager (PMI) covering 6.8 GHz to 150 GHz bands with a 1.8 m diameter reflector antenna for conical scan. Most of its frequency channels have the capability of full-polarizations. Observations of this sensor can retrieve parameters such as temperature, rain and water vapor. It also can help to do atmosphere correction and build a bridge to historical data. The third payload is an X-Ku dual-frequency polarized scatterometer (DPS) with 2~5 km resolution and 1000 km swath. This scatterometer is designed for snow water equivalent and freeze/thaw.

One objective of WCOM is to improve the resolution of soil moisture product. For passive downscaling, one of the three payloads onboard the WCOM, IMI can provide observations at L, S and C bands with spatial resolution of 50 km, 30 km and 15 km, at varying incidence angles along the cross-track direction. Multi-frequency multi-angle remote sensing observations from IMI provide an efficient way to downscale TB and soil moisture, accounting for the vegetation effects and potentially avoiding the issues caused by RFI. It allows us to obtain higher resolution TB and soil moisture using downscaling method in two ways: 1) downscaling L-band TB (50 km) using S-band TB (30 km). 2) downscaling L-band TB (50 km) using C-band TB (15 km). We can obtain higher resolution soil moisture by retrieving the downscaled L-band TB with the higher resolution same to the resolution of S-band or C-band observations, which would then benefit to various applications. In this research, we mainly present the first downscaling method using L-band and S-band.

III. STUDY AREA AND DATA

As of 2017, there is no satellite dataset of S-band radiometer, and there are few large scale L-band and S-band radiometer datasets available to test the method developed for WCOM in this research. Available data are the Passive and Active L-band System (PALS) data from SGP99, SMEX02, CLASIC, and SMAPVEX08 fields experiments[13][14]. Finally, we selected the PALS datasets from SMEX02 to evaluate the performance of the algorithm proposed in this research. The advantage of SMEX02 PALS dataset is that there are wet and dry soil moisture conditions within the PALS flight domain for the campaign duration. The PALS L-band and S-band radiometer have similar frequencies to WCOM, but the PALS instruments have much finer spatial resolution approximately 400 m depending on flight altitude. To test the algorithm using PALS data, the PALS data were resampled to 800 m and 4km.

A. Study Area

The Soil Moisture Experiments in 2002 (SMEX02) was conducted in Walnut Creek Watershed in one month period between mid-June and mid-July in 2002[15][16]. Walnut Creek Watershed is a small watershed located south of Ames, IA, USA. Nearly 75% of the region is used for row crop agriculture with corn and soybeans being the main crops. The climate is humid with an annual rainfall of 835 mm. The figure (Fig 1) is the SMEX02 Walnut Creek watershed area and microwave aircraft flightlines[17].

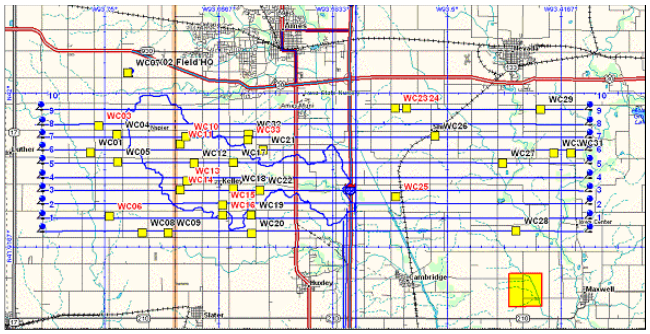

Fig1 SMEX02 Walnut Creek watershed area and microwave aircraft flightlines. Blue lines are the low altitude microwave flightlines; yellow squares indicate intensive soil moisture sampling sites (those with red text are also flux tower sites). The large yellow square is 2 km by 2 km and is used to illustrate scale.

B. PALS Data

The PALS has microwave radiometer operating at 1.41GHz (L-band) and 2.69 GHz (S-band) with multiple polarizations, with the angle of incidence being 45 °[18]. During SMEX02, the PALS instrument was flown on a C-130 aircraft at an altitude of 1 km, on June 25 and 27, 2002 and July 1, 2, and 5–8, 2002, over the watershed study area. There were 8 days of data in total.

The spatial coverage of flight lines is about 50km × 10km. The instrument sampled a single footprint track along the flight path, with each sample having a footprint resolution of approximately 330m × 470 m. We removed the data on July 1st from the process and the analysis, since there are only four flight lines because of a problem of experimental instrument. We finally use 7 days of data in the downscaling process.

C. Field Measurements

In situ measurements of soil moisture and ancillary data such as soil temperature, soil text, vegetation water content, and soil bulk density were carried out over 31 field sampling sites (yellow squares in Fig 1) coincidently with PALS observations. We removed the data on July 2nd from the validation process because there was no *in situ* sampling data on this day.

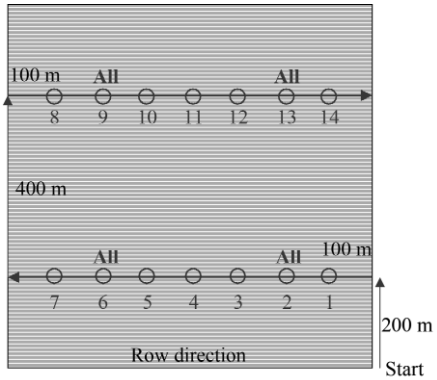

Fig.2 The layout of the sampling plan in SMEX02

Each sampling site covers approximately an 800 m ×800 m rectangle area as shown in Fig.2. Volumetric soil moisture (vsm) (0–6cm) of the sample sites was synchronously measured with a Delta-T Theta Probe at the 14 sample points. Average soil moisture for each of the sites was computed by averaging the data collected from 14 sample points on each sampling date. Gravimetric soil moisture, soil bulk density and the soil temperature samples were only taken at four points, marked "All".

Soil temperature is an important parameter in retrieval of soil moisture. However, we cannot get synchronous temperature sampling data with the airborne PALS TB observation. The time difference between the sampling temperature and the PALS observations can be 2 or 3 hours, bring out the temperature change during this period can be 10℃ to 20℃. So the sampling temperature cannot be used in soil moisture retrieval. A total of 10 meteorological stations were deployed across the sampling domain, which provided the synchronous temperature data with the PALS observations. Air temperature and infrared skin temperatures were measured for the duration of the experiment at each station[19].

Combined temperature data from those 10 meteorological stations with ancillary data from 10 sampling sites in the same location can provide all the information necessary to evaluate the soil moisture algorithm at the surface. We removed 3 sites which are mixed pixels in the resampled TB data. We finally used 7 sites field data to retrieve soil moisture.

IV. DOWNSCALING METHODOLOGY

L-band is considered to be the most suitable frequency for soil moisture[20]. For sensor configuration of WCOM, L-band can retrieve soil moisture with high accuracy but it has lower resolution (50 km) than S-band (30 km). The principle of this downscaling method is using S-band TB with higher resolution to downscale L-band TB, based on the linear relationship of TB between these two bands. Then we can retrieve soil moisture products with higher resolution using downscaled L-band TB. A vegetation index is adopted to correct the vegetation effects in the linear relationship. The flow chart is shown in Fig 3.

Based on the footprint resolution(330m × 470 m.), sampling site spatial coverage(800 m ×800 m ,described in part C Field Measurements of section 3) and the experience of previous researchers[16], we did the TB data preprocessing. The 7 days of PALS TB data both at H and V polarizations were resampled to a spatial resolution of 800 m and averaged to 4 km as needed.

For the convenience of description, we set the resolution of L band as coarse scale(C), while set the resolution of S band as medium scale(M). The corresponding resolution of C is 50km in satellite and 4km in PALS data, while he corresponding resolution of M is 30km in satellite and 800m in PALS data, as shown in Table 2:

Table 2. Resolution of L band and S band

Resolution	WCOM/IMI	SMEX02/PALS
C(L-band)	50km	4km
M(S-band)	30km	800m

As shown in the flow chart Fig 3, the downscaling process has following 4 steps:1)Data preprocessing: we resampled the SMEX02 PALS data to resolution of 800m, and averaged them to 4km. 2) Build linear relationship: based on TB data at 4km, we built the linear relationship of TB between these two bands.

3) Downscaling: with the TBS at 800m and the relationship, we got the TBL at 800m, namely the downscaled results. 4) Validation: we validated the downscaled TBL at 800m by comparing it with the observed TBL at 800m.

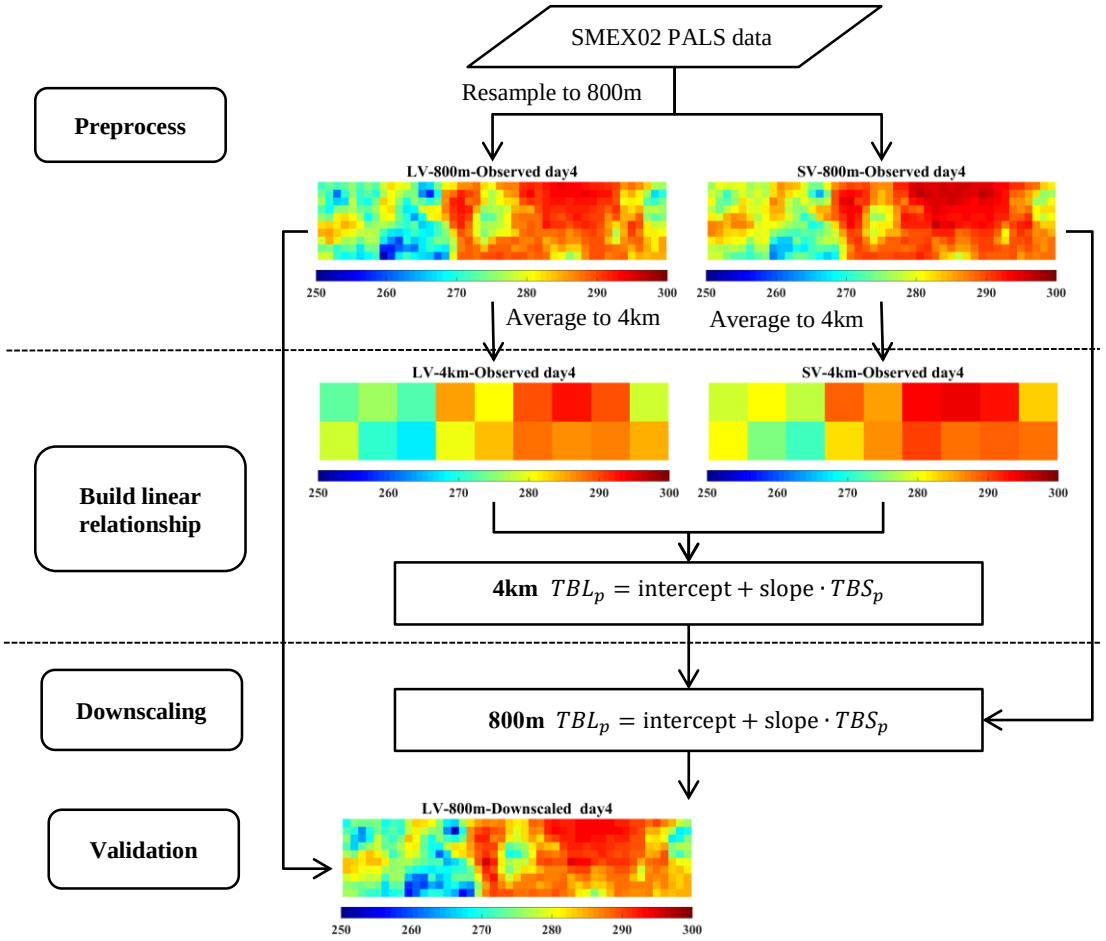

Fig 3 Flow chart .of downscaling method

A. Theoretical basis

When modeling the microwave radiation transfer model, especially in low frequency such as L-band and S-band, the multiple scattering effects of vegetation layer are often ignored and the zeroth order approximation model is adopted as follows:

$$E_p^t = F_v \cdot E_p^v + F_v \cdot E_p^v \cdot R_p^e \cdot L_p + F_v \cdot E_p^s \cdot L_p + (1 - F_v) \cdot E_p^s \quad (1)$$

Where E is the emissivity and $L = \exp(\frac{-\tau}{\cos(\theta)})$ is the one-way attenuation factor. θ is sensor viewing angle and τ is the optical thickness of vegetation canopy. The superscripts v and s indicate the vegetation and soil components and the subscript p is polarization status. The emissivity of the vegetation canopy is given by $E_p^v = (1 - \omega_p) \cdot (1 - L_p)$. $R_p^e = 1 - E_p^s$ is the surface effective reflectivity.

Based on $\tau - \omega$ model in equation (1), radiative transfer equation can be simplified to the vegetation transmission component V_p^t and the vegetation emission component V_p^e[21]

$$TB_p = V_p^e \cdot T_v + E_p^s \cdot V_p^t \cdot T_s \quad (2)$$

Bare surface emissivities at L-band and S-band are highly correlated and can be approximated as an equal at a given polarization[21], namely $E_p^s(L) \approx E_p^s(S)$, so

$$\frac{E_p^t(L) - V_p^e(L)}{V_p^t(L)} = E_p^s(L) \approx E_p^s(S) = \frac{E_p^t(S) - V_p^e(S)}{V_p^t(S)} \quad (3)$$

$$E_p^t(L) = \left[V_p^e(L) - \frac{V_p^t(L)}{V_p^t(S)} \cdot V_p^e(S)\right] + \frac{V_p^t(L)}{V_p^t(S)} \cdot E_p^t(S) \quad (4)$$

Finally, we deduced the following linear relationship between TB of L band (TBL) and TB of S band (TBS):

$$TBL_p = \left[V_p^e(L) - \frac{V_p^t(L)}{V_p^t(S)} \cdot V_p^e(S)\right] \cdot T_v + \frac{V_p^t(L)}{V_p^t(S)} \cdot TBS_p \quad (5)$$

Namely,

$$TBL_p = a + b \cdot TBS_p \quad (6)$$

B. Vegetation correction

The vegetation signal changes temporally in agricultural domains, especially during the growing season. In order to find a more accurate description of the relationship between TBL and TBS, we adopt the microwave vegetation index (MVI)[22], which is sensitive to vegetation and surface features, to correct the linear equation:

$$\mathrm{MVI} = \frac{TBS_v - TBS_h}{TBL_v - TBL_h} \quad (7)$$

$$TBL_p = (\mathrm{a} + \mathrm{c} \cdot \frac{\mathrm{MVI^t}}{\overline{\mathrm{MVI}}^{\mathrm{t}}}) + (\mathrm{b} + \mathrm{d} \cdot \frac{\mathrm{MVI^t}}{\overline{\mathrm{MVI}}^{\mathrm{t}}}) \cdot TBS_p \quad (8)$$

Where, $\overline{\mathrm{MVI}}^{\mathrm{t}}$ is the mean value of MVI within the time sequence t. According to the sensor configuration, the resolution of passive L band is coarse scale (C) and the resolution of S band is medium scale (M). So the equation (8) at coarse scale(C) is:

$$TBL_p(C) = (\mathrm{a(C)} + \mathrm{c(C)} \cdot \frac{\mathrm{MVI^t}}{\overline{\mathrm{MVI}}^{\mathrm{t}}}) + (\mathrm{b(C)} + \mathrm{d(C)} \cdot \frac{\mathrm{MVI^t}}{\overline{\mathrm{MVI}}^{\mathrm{t}}}) \cdot TBS_p(C) \quad (9)$$

Namely,

$$TBL_p(\mathrm{C}) = \mathrm{Intercept} + \mathrm{Slope} \cdot TBS_p(\mathrm{C}) \quad (10)$$

Where $TBS_p(C) = 1/nm \sum_{nm}^{i=1} TBS_p(M_i)$, is the average value of medium grids in grid C, and M_i is the medium grid and the nm is the number of M grids within grid C. In equation 10, $\mathrm{Intercept} = \mathrm{a} + \mathrm{c} \cdot \frac{\mathrm{MVI^t}}{\overline{\mathrm{MVI}}^{\mathrm{t}}}$, and $\mathrm{Slope} = \mathrm{b} + \mathrm{d} \cdot \frac{\mathrm{MVI^t}}{\overline{\mathrm{MVI}}^{\mathrm{t}}}$.

At coarse scale, we statistically estimated coefficients a, b, c, and d through regression time sequence observations in grid C. The slope and the intercept relating to TBL and TBS, mainly rely on vegetation and soil roughness characteristics. So they vary as the seasons change and land cover evolves. Scientists estimated the time window as 6-8 months for croplands when they researched the sensitivity of active and passive L-band observations temporal covariance to land surface characteristics[23]. For a particular research area and in a short period of time, the vegetation and surface roughness can be considered constant, so the slope and intercept is constant at coarse scale C and at medium scale M.

C. Slope adjustment and L-band TB downscaling

After the vegetation correction, the values of slope have a larger range, which may exceed the reasonable range. To avoid some abnormal values of slope, we calculated the cumulative distribution function (CDF) and adjusted the slope range by limiting slope values from 5% CDF to 95% CDF. We seted the slope values that were out of range as the minimum or the maximum value of the slope CDF boundary values.

At medium scale (M), we applied the relationship to the TBS at medium resolution ($TBS_p(M)$), and obtained the target of this algorithm, namely, the downscaled TBL ($TBL_p(M)$), using the adjusted coefficients slope:

$$TBL_p(\mathrm{M}) = \mathrm{Intercept} + \mathrm{Slope} \cdot TBS_p(\mathrm{M}) \quad (11)$$

The complete formula is

$$TBL_p(M) = (\mathrm{a(C)} + \mathrm{c(C)} \cdot \frac{\mathrm{MVI^t}}{\overline{\mathrm{MVI}}^{\mathrm{t}}}) + (\mathrm{b(C)} + \mathrm{d(C)} \cdot \frac{\mathrm{MVI^t}}{\overline{\mathrm{MVI}}^{\mathrm{t}}}) \cdot TBS_p(M) \quad (12)$$

To ensure that the downscaled TB from this algorithm $TBL_p(\mathrm{M})$ is consistent with the original observed TBL at scale C, the bias in $TBL_p(M)$ was removed by imposing:

$$TBL_p(C) = 1/nm \sum_{nm}^{i=1} TBL_p(M_i) \quad (13)$$

D. Soil moisture retrieval

The disaggregated L-band TB $TBL_p(M)$ and the observed L-band TB were then used to retrieve surface soil moisture at medium scale, using single channel retrieval algorithm(SCA)[24] with ancillary data in SMEX02.

The parameters used in SCA for soil moisture retrieval were as follows. For the vegetation parameters, single-scattering albedo was taken as 0.05 for both soybeans and corn. The vegetation opacity coefficient, b, between vegetation water content and the opacity, was taken as 0.16 for soybean and 0.05 for corn at L band. For the soil parameters, the roughness parameter, h, was set as 0.1 for V polarization and 0.6 for H polarization, for both soybeans and corn. The polarization mixing parameter Q, was taken as zero[25]. The dielectric model of the soil water mixture used in this research was the Mironov model[26]. *In situ* measurements of soil moisture, land surface temperature, bulk density, and vegetation water content during the SMEX02 experiments were downloaded from the National Snow and Ice Data Center (NSIDC).

V. RESULTS

At coarse scale (4 km), we regressed relationship coefficients in Equation (9) through the time sequence observations on each coarse grid C. We limited the range of slope values according to CDF. Then we used the regression equation and coefficients to obtain the downscaled TBL with TBS at medium scale (800 m). The steps were, (a) established and adjusted the linear relationship at coarse resolution (C) using PALS data, (b) downscaled TBL using TBS and results validation at medium resolution, and (c) soil moisture retrieval with downscaled TBL at medium resolution.

A. Establish and adjust linear relationship at coarse resolution Using PALS Data

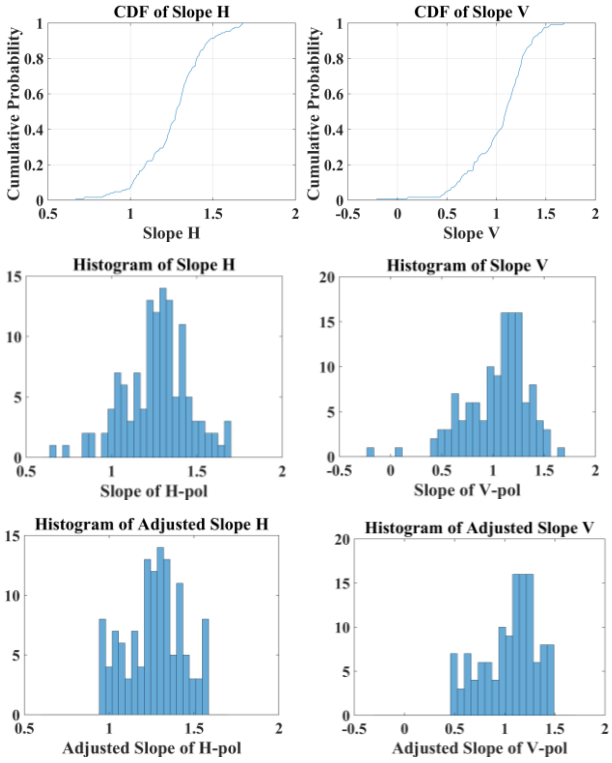

Fig 4 CDF, histogram of slopes and adjusted slopes at coarse scale for H-polarization (left column) and V- polarization (right column).

The regression procedure described previously was carried out using PALS radiometer data in SMEX02 at a coarse resolution of 4 km. The CDF and histogram of slope at 4 km resolution were displayed in Fig 4. As shown in the figures in the middle row, there are some abnormal slopes, and it even appears negative values. To make the results more reasonable, the slopes were limited from 5% CDF to 95% CDF. The adjusted slopes are shown in Fig 4. For H-polarization (left column), the slopes were limited from 0.9513 to 1.5697, and for V-polarization (right column), the slopes were limited from 0.5176 to 1.4445. After slope adjustment, we removed the abnormal values of slopes and made the slope values in a more reasonable range.

B. Downscaling TBL using TBS and results validation at medium resolution

We used PALS TBL and TBS data in SMEX02 experiment to validate the downscaling method. The downscaling results are shown in Fig 5 and Fig 6. Fig 5 is the downscaling results of TBL with TBS and Fig 6 is the scatterplot of downscaling results against the original observations of L band at 800 m resolution..

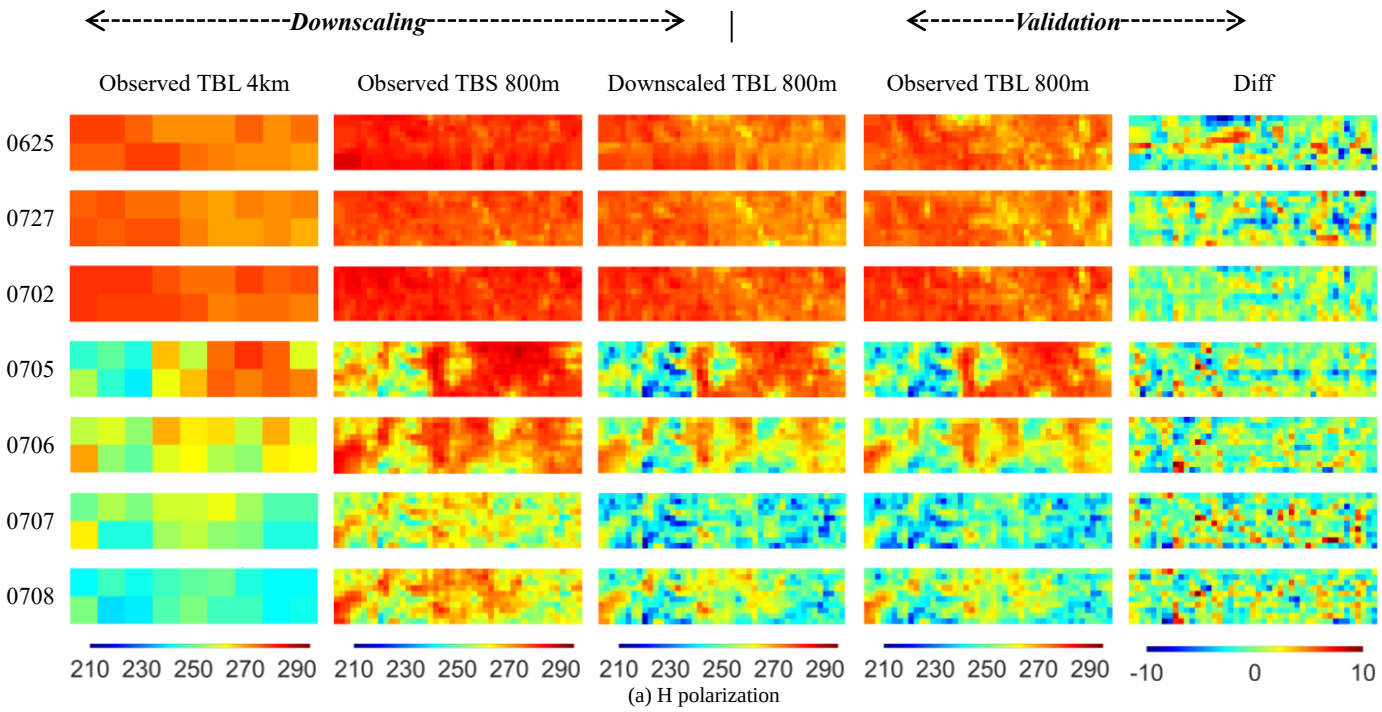

(a) H polarization

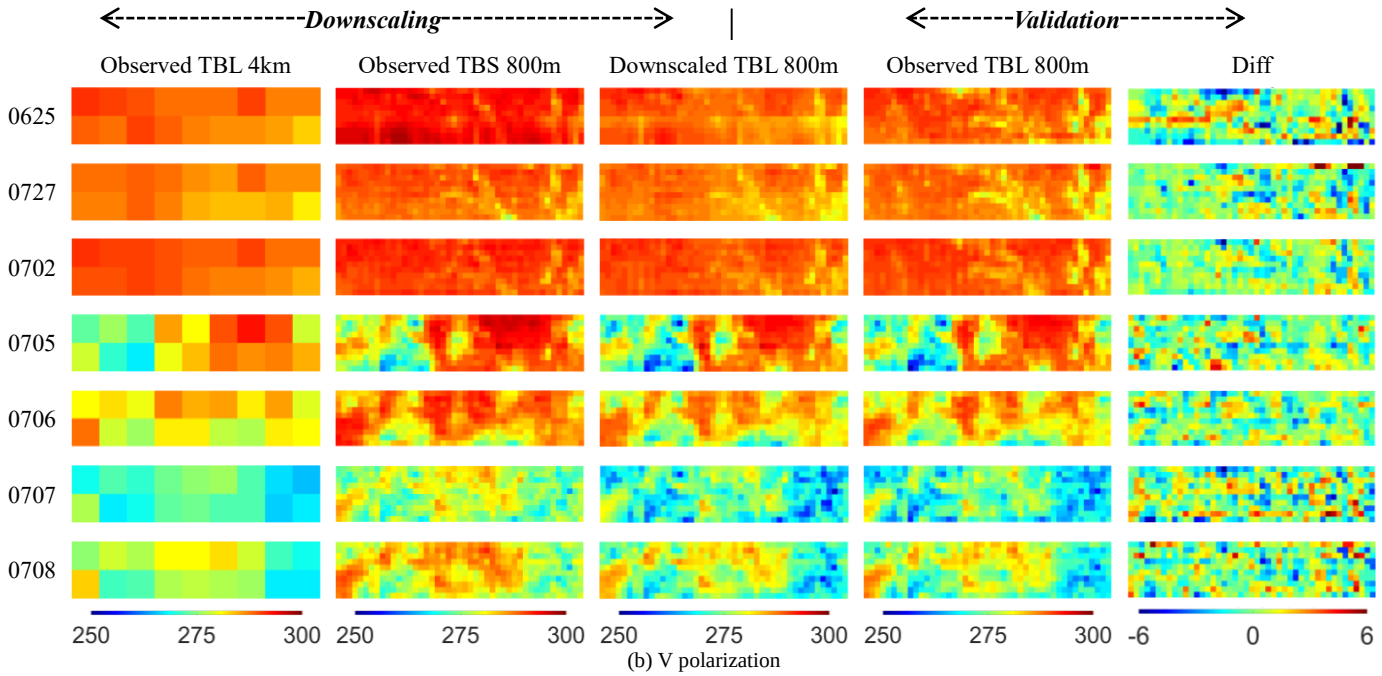

(b) V polarization

Fig 5 Downscaling results of TBL using TBS (a) H polarization (b) V polarization (from left to right, original TBL observations at 4 km, observed TBS at 800m, downscaled TBL at 800 m, original TBL observations at 800 m, and the differnce between the observed and the downscaled TBL at 800m, respectively)

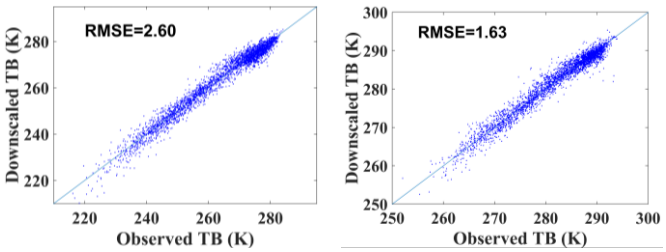

(a) H polarization (b) V polarization

Fig 6 The scatterplot of downscaled TBL versus original TBL observations at 800 m: (a) H polarization and (b) V polarization.

Fig 5 shows the downscaling results of TBL using TBS data for H polarization and V polarization, from Jun 25 to Jul 8,2002. For the downscaling process, we use the observed TBL at 4km (the first column) and observed TBS at 4km establish the relationship, then use the observed TBS at 800m (the second column) to get the downscaled TBL at 800m (the third column). For validation, we compare the downscaled TBL at 800m with the observed TBL at 800m (the last column), and the difference between them is displayed in the last column.

In Fig 5 we can see that there was rainfall event during the experiment. The downscaled TBL at 800 m resolution can basically present the spatial distribution condition of observed TBL at 800 m resolution, and has more detail heterogeneity in grid C than that of the observed TBL at 4 km. It's obvious that the downscaled TBL effectively captured the rainfall event and had more spatial distribution details. Of course the downscaling process cannot reproduce the high resolution TBL. There are some differences between them, as shown in the last column of Fig 5. By comparison, the downscaling difference is bigger when the spatial heterogeneity is greater within a coarse grid.

From the view of precision, as displayed in scatterplots in Fig 6, the root mean square errors (RMSE) between the downscaled TBL at 800m with the observed TBL at 800m are 2.60 K and 1.63 K for H polarization and V polarization respectively. The RMSE between the observed TBL at 4 km and the observed TBL at 800 m are 6.33 K and 3.44 K for H/V polarization respectively. The improvement from 6.33 to 2.60 K and the improvement from 3.44 to 1.63 K are partly because of the higher resolution observation of TBS, and are partly because of the consideration of vegetation and surface roughness heterogeneity within grid C, with the correction of MVI. The higher resolution of the downscaled TBL enables the soil moisture retrieval at resolution M, which is presented in next paragraph.

C. Soil Moisture Retrieval Results and Validation

Surface soil moisture retrievals of the disaggregated TBL at 800 m were implemented, using the SCA[24] with ancillary data from SMEX02 and tower based data[27][28].

Fig 7 and Fig 8 are plots and time series plots of soil moisture retrieved from PALS TBL versus the in situ soil moisture in the 5 cm soil layer (a) at horizontal polarization and (b) at vertical polarization, in which from top to bottom are results for the downscaled TBL at 800m resolution and observed PALS TBL at 800m resolution. In the aspect of precision displayed in Fig 7, at H polarization, the RMSE are 0.0576 m^3/m^3 and 0.0593 m^3/m^3 for the downscaled TBL and for the observed TBL, respectively. At V polarization, the RMSE are 0.0308 m^3/m^3 and 0.0318 m^3/m^3 for the downscaled TBL and for the observed TBL, respectively, though these are not significantly different with a significance level of 5% (p-value of 0.89). As shown in Fig 8, the SCA-V performs better than the SCA-H. At H polarization, the main source of RMSE is the first several dry days. The retrieved soil moisture has an underestimation compared with the in situ soil moisture.

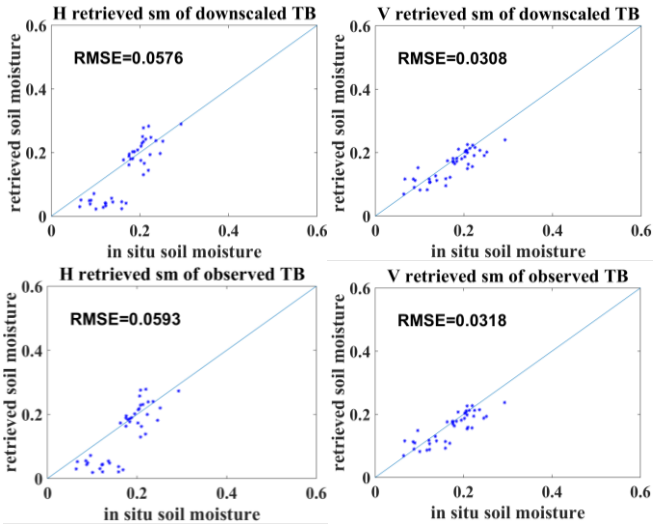

(a) H-pol (b) V-pol

Fig 7 Scatter plots of retrieved soil moisture versus *in situ* soil moisture measured in the 5cm soil layer at (a)H-pol, and at (b) V-pol. From top to bottom are the results of downscaled TBL at 800m resolution and the observed TBL at 800m resolution.

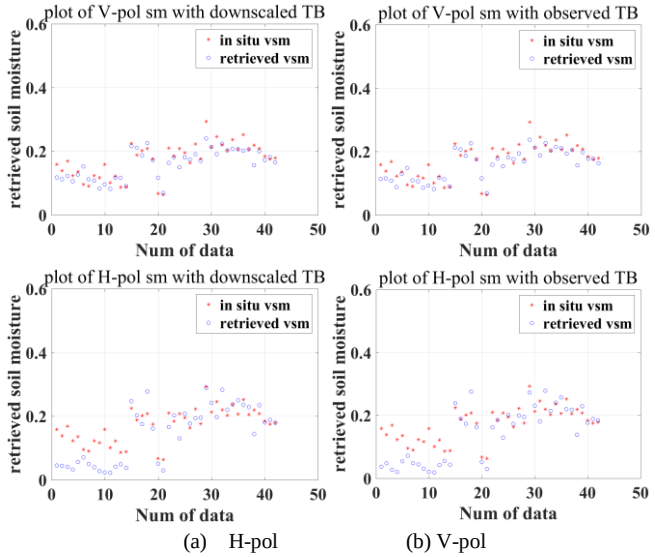

(a) H-pol (b) V-pol

Fig 8 time series plots of retrieved soil moisture versus *in situ* soil moisture measured in the 5cm soil layer over at (a) H-pol, and at (b) V-pol. From top to bottom are the results for the downscaled TBL at 800m resolution and the observed TBL at 800m resolution.

The SCA-V performs better than the SCA-H in our study, which is consistent with the validation of SMAP-L2SMP products[29]. The RMSEs at H polarization are higher than the expected accuracy. Some errors may be caused by setting roughness parameter h and single scattering albedo ω as fixed

values, irrespective of differences between the soil and vegetation conditions.

VI. DISCUSSION

We developed this downscaling method for future satellite mission WCOM. Since there is no satellite dataset of S-band radiometer, we selected the PALS datasets from SMEX02 field flight experiment to evaluate the performance of the algorithm proposed in this research. Now there is no similar downscaling method with L band and another passive band(such as S band or C band). A similar downscaling method is the SMAP active/passive downscaling method. They built a linear relationship between the L band passive TB and the L band active signal sigma. In the SMAP handbook [30]:

$$\mathrm{TB} = \alpha + \beta * \sigma \tag{14}$$

Our downscaling concept are similar to that of SMAP downcaling method. We used S band radiometer TB to downscale L band radiometer TB, while the SMAP used L band radar observations to downscale the L band radiometer observations. For the vegetation effects , we adopted the microwave vegetation index (MVI) derived from L band and S band TB to correct the relationship, while the SMAP used a heterogeneity indicator derived from cross-polarization backscatter σ_{hv} to indicate the subgrid heterogeneity in vegetation and surface physical characteristics.

The performance of SMAP algorithm was evaluated using the PALS dataset from SMEX02. The RMSE of the TB disaggregation at V polarization is 1.8K(4 km to 0.8 km). When they resampled the 4 km radiometer data to 0.8 km, the RMSE is 2.75K. So they improved the 2.75K to 1.8K by downscaling. In our research, the RMSE of the TB disaggregation are 2.60 K and 1.63 K for H polarization and V polarization respectively. When we resampled the 4 km radiometer data to 0.8 km, the RMSE are 6.33 K and 3.44 K for H/V polarization respectively. Our improvement is from 6.33K to 2.60 K and from 3.44 to 1.63 K for H/V polarization . So through the downscaling using the TBS, we get a comparable result with the performance of SMAP downscaling method. The improvement in those two methods, are partly because of the higher resolution observation of TBS or the radar observations, and are partly because of the consideration of vegetation and surface roughness heterogeneity.

In this research, the L-band and S-band data are assumed to be "simply" linearly correlated, similar "simple" assumption is also made for the SMAP mission, as shown in equation(14). It is not so simple that the coefficients can change according to the ground conditions especilly the vegetation dynimics and the configuration of observations. Things are more complex as the 1-D synthetic apture sensor IMI of WCOM obtain TB observations at varying incidence angles. Thus, people can apply the SCA or DCA algorithm to S-band, C-band for retireving soil moisture, but need to deal with parameters calibration. And another option, as proposed in this manuscript, is to downscale the S-band and C-band data to L-band, so that the same algorithm and parameters could be implemented.

VII. CONCLUSION

According to the passive configuration of WCOM, we developed an L-band TB downscaling method with S-band passive measurements, and obtained soil moisture products with higher resolution. The results showed that, with S-band TB observations at 30 km resolution, L-band TB observations of WCOM at 50 km resolution can be downscaled to a higher resolution (30km) and be retrieved to surface soil moisture. This method took advantages of the resolution of S-band TB and the advantages of the sensitivity to the soil moisture of L-band TB. Based on the similar emissivity, we established a linear relationship between these two bands signals. TB downscaling and soil moisture retrieval using this algorithm were performed using PALS data in SMEX02. The results indicate that it is possible to produce soil moisture estimates with high accuracy and higher resolution using observations of WCOM, which has a high science value and will benefit various applications. The results also showed that it was possible to use these disaggregated TB to estimate soil moisture to meet the WCOM mission requirement of 0.04 m^3/m^3.

ACKNOWLEDGMENT

This work was supported in part by the National Key Basic Research Program (2015CB953701), Key Research Program of Frontier Sciences, CAS (Grant No. QYZDY-SSW-DQC011), International S&T Cooperation Program of China (2016YFE0117300), the National Natural Science Foundation of China (41371354, 41301396) and the Youth Innovation Promotion Association (No.2016061). The University of Chinese Academic of Science (UCAS) Joint PhD Training Program is acknowledged. The authors would like to acknowledge NSIDC for providing the SMEX02 experiments datasets. USDA is an equal opportunity provider and employer.

REFERENCES

[1] V. Lakshmi, T. Piechota, U. Narayan, and C. Tang, "Soil moisture as an indicator of weather extremes," *Geophysical Research Letters*, vol. 31, no. 11, pp. 2–5, 2004.

[2] T. G. Caldwell, E. V. McDonald, and M. H. Young, "Soil disturbance and hydrologic response at the National Training Center, Ft. Irwin, California," *Journal of Arid Environments*, vol. 67, no. 3, pp. 456–472, 2006.

[3] B. P. Mohanty and T. H. Skaggs, "Spatio-temporal evolution and time-stable characteristics of soil moisture within remote sensing footprints with varying soil, slope, and vegetation," *Advances in Water Resources*, vol. 24, no. 9–10, pp. 1051–1067, 2001.

[4] S. B. Kim, L. Tsang, J. T. Johnson, S. Huang, J. J. Van Zyl, and E. G. Njoku, "Soil moisture retrieval using time-series radar observations over bare surfaces," *IEEE Transactions on Geoscience and Remote Sensing*, vol. 50, no. 5 PART 2, pp. 1853–1863, 2012.

[5] Y. H. Kerr *et al.*, "The SMOS Mission:New Tool for Monitoring Key Elements of the Global Water Cycle," *Proceedings of the IEEE*, vol. 98(5), pp. 666–685, 2010.

[6] Y. H. Kerr, P. Waldteufel, J. P. Wigneron, J. M. Martinuzzi, J. Font, and M. Berger, "Soil moisture retrieval from space: The Soil Moisture and Ocean Salinity (SMOS) mission," *IEEE Transactions on Geoscience and Remote Sensing*, vol. 39, no. 8, pp. 1729–1735, 2001.

[7] D. M. Le Vine, L. G.S.E., R. Colomb, Yueh Simon, and P. F., "Aquarius : An Instrument to Monitor Sea Surface Salinity from Space," *IEEE Transactions on Geoscience and Remote Sensing*, vol. 45(7), pp. 2040–2050, 2007.

[8] R. Bindlish, T. J. Jackson, M. H. Cosh, T. Zhao, and P. E. O'Neill, "Global soil moisture from the Aquarius satellite description and initial assessment," *IEEE Geoscience and Remote Sensing Letters*, vol. 12, no. 5, pp. 923–927, 2013.

[9] D. Entekhabi *et al.*, "The soil moisture active passive (SMAP) mission," *Proceedings of the IEEE*, vol. 98(5), pp. 704–716, 2010.

[10] B. Fang and T. J. Jackson, "Passive Microwave Soil Moisture Downscaling Using Vegetation Index and Skin Surface Temperature," 2013.

[11] J. Shi *et al.*, "WCOM : The science scenario and objectives of a global water cycle observation mission," *Geoscience and Remote Sensing Symposium (IGARSS), 2014 IEEE International*, pp. 3646–3649, 2014.

[12] X. Dong, H. Liu, Z. Wang, J. Shi, and T. Zhao, "WCOM: The mission concept and payloads of a global water cycle observation mission," *Geoscience and Remote Sensing Symposium (IGARSS), 2014 IEEE International*, pp. 3338–3341, 2014.

[13] B. P. Mohanty, T. H. Skaggs, and J. S. Famiglietti, “Analysis and mapping of field-scale soil moisture variability using high-resolution, ground-based data during the Southern Great Plains 1997(SGP 97) Hydrology Experiment,” *Water Resources Research*, vol. 36, no. 4, pp. 1023–1031, 2000.
[14] A. Colliander *et al.*, “Long term analysis of PALS soil moisture campaign measurements for global soil moisture algorithm development,” *Remote Sensing of Environment*, vol. 121. pp. 309–322, 2012.
[15] U. Narayan, V. Lakshmi, and T. J. Jackson, “High-resolution change estimation of soil moisture using L-band radiometer and radar observations made during the SMEX02 experiments,” *IEEE Transactions on Geoscience and Remote Sensing*, vol. 44, no. 6. pp. 1545–1554, 2006.
[16] U. Narayan, V. Lakshmi, and E. G. Njoku, “Retrieval of soil moisture from passive and active L/S band sensor (PALS) observations during the Soil Moisture Experiment in 2002 (SMEX02),” *Remote Sensing of Environment*, vol. 92, no. 4. pp. 483–496, 2004.
[17] SMEX02, “Soil Moisture Experiments in 2002(SMEX02) Summary of Experiment Plan.” 2002.
[18] W. J. Wilson *et al.*, “Passive active L-and S-band (PALS) microwave sensor for oceansalinity and soil moisture measurements,” *Geoscience and Remote Sensing, IEEE Transactions on*, vol. 39, no. 5. pp. 1039–1048, 2001.
[19] J. Prueger *et al.*, “SMEX02 SMACEX Tower Meteorological/Flux Data: Iowa.” Boulder,Cororado USA: NASA DAAC at the National Snow and Ice Data Center, 2009.
[20] E. G. Njoku and D. Entekhabi, “Passive microwave remote sensing of soil moisture,” *Journal of Hydrology*, vol. 184, no. 1–2, pp. 101–129, 1996.
[21] J. Shi, E. G. Njoku, T. Jackson, P. O. Neill, and K. S. Chen, “Estimation of soil moisture with dual-frequency-PALS,” *Geoscience and Remote Sensing Symposium (IGARSS), 2008 IEEE International*, vol. 2, pp. 73–76, 2008.
[22] J. Shi *et al.*, “Microwave vegetation indices for short vegetation covers from satellite passive microwave sensor AMSR-E,” *Remote Sensing of Environment*, vol. 112, no. 12. pp. 4285–4300, 2008.
[23] M. Piles *et al.*, “Sensitivity of Aquarius Active and Passive Measurements Temporal Covariability to Land Surface Characteristics,” pp. 1–12, 2015.
[24] T. J. Jackson, “measuring surface soil moisture using passive microwave remote sensing,” *hydrological process*, vol. 7, pp. 139–152, 1993.
[25] J.-P. Wigneron, L. Laguerre, and Y. H. Kerr, “A simple parameterization of the L-band microwave emission from Rough agricultural soils,” *IEEE Transactions on Geoscience and Remote Sensing*, vol. 39, no. 8. pp. 1697–1707, 2001.
[26] V. Mironov, Y. Kerr, J. P. Wigneron, L. Kosolapova, and F. Demontoux, “Temperature-and texture-dependent dielectric model for moist soils at 1.4 GHz,” *IEEE Geoscience and Remote Sensing Letters*, vol. 10, no. 3. pp. 419–423, 2013.
[27] T. Jackson, M. Cosh, W. P. Dulaney, and McKee L., “SMEX02 Land Surface Information: Geolocation, Surface Roughness, and Photographs, Version 1,” *Boulder, Colorado USA. NASA National Snow and Ice Data Center Distributed Active Archive Center.*, 2004. [Online]. Available: https://nsidc.org/data/NSIDC-0204/versions/1.
[28] D. Miller, “SMEX02 Land Surface Information: Soils Database, Version 1,” *Boulder, Colorado USA. NASA National Snow and Ice Data Center Distributed Active Archive Center.*, 2006. [Online]. Available: https://nsidc.org/data/NSIDC-0278/versions/1.
[29] T. J. Jackson *et al.*, “Soil Moisture Active Passive(SMAP) Project Calibration and Validation for the L2/3_SM_P Beta-Release Data Products Version 2,” Pasadena,CA, 2015.
[30] D. Enrekhabi *et al.*, “SMAP handbook–soil moisture active passive: Mapping soil moisture and freeze/thaw from space,” *Mapping Soil Moisture and Freezs/Thaw from Space*. p. 192, 2014.